ELASTIC ELECTRON SCATTERING FROM ^{3}He AND ^{4}He[*]
AT HIGH MOMENTUM TRANSFER

R. G. Arnold, B. T. Chertok, S. Rock, W. P. Schütz,[†] and Z. M. Szalata
American University, Washington, D. C. 20016

D. Day and J. S. McCarthy
University of Virginia, Charlottesville, Va. 22901

F. Martin
Stanford Linear Accelerator Center, Stanford, Ca. 94305

B. A. Mecking
Universität Bonn, Bonn, Germany

I. Sick
Universität Basel, Basel, Switzerland

G. Tamas
Centre d'Etudes Nucleaires de Saclay, Gif-sur-Yvette, France

ABSTRACT

Experimental values of ^{3}He (^{4}He) elastic structure functions up to momentum transfer $q^2 = 4.0$ (2.4) $(GeV/c)^2$ are presented. They are compared to calculations using three- and four-body wave functions and to asymptotic models.

(Submitted to Phys. Rev. Lett.)

We present data on elastic electron scattering from ^{3}He and ^{4}He that extends the information from previous experiments[1] into the unexplored region of momentum transfer $q^2 > 0.8$ (GeV/c)^2. This complements the high q^2 measurements of the electromagnetic structure functions already available for the deuteron[2] by a study of two other basic few-nucleon systems. High q^2 data measures the nuclear density with better spatial resolution ($\approx 1.5/q_{max}$) and may allow a better understanding of the failure of microscopic calculations[3-11] to explain existing data near $q^2 = 0.8$ (GeV/c)^2. High q^2 data also will be important for an understanding of the asymptotic behavior of the structure functions. For example, in the dimensional-scaling-quark model (DSQM) the structure functions at large q^2 are predicted[12] to decrease according to a power of q^2 determined by the number of elementary constituents. This is consistent with experiment for π, p, n, and d structure functions. Of particular interest is the determination of the momentum transfer of the onset of this scaling. A high q experiment therefore may investigate the region of the transition from nuclear to elementary-particle physics.

The experiment was performed at the Stanford Linear Accelerator Center using high pressure gas targets and the 20- and 8-GeV spectrometers to detect the scattered electrons and the recoil nuclei in coincidence. The target cells were designed to achieve high density and high heat extraction rate while maintaining a small window thickness in the direction of the recoiling He nuclei. A 42 cm long cell with 0.4 mm Al windows was used at 50 atm pressure. The gaseous He was circulated through a heat exchanger cooled with liquid hydrogen to remove the 150 W deposited by the $15\,\mu$A average beam current. This target

system contained a total of 2000 liters (STP) of ^{3}He (isotopic purity 98.2% with 1.8% ^{4}He) yielding a total target thickness of 3 g/cm^2. A 10 atm target cell with 0.094 mm Al windows was used for the lowest q^2 points.

The scattered electrons of 6 to 15 GeV were detected at 8$^{\text{o}}$ in the SLAC 20-GeV spectrometer[13]. Electrons were identified and measured by three plastic scintillators, a total absorption shower counter, a nitrogen gas Cerenkov counter and by 5 planes of proportional wire chambers. To separate elastic from inelastic scattering the recoiling He nuclei were detected in coincidence with the scattered electrons. Single arm electron measurements with a resolution of 0.5% due to the beam energy spread could not resolve the elastic peak from the quasielastic spectrum (breakup threshold in ^{3}He is 5.5 MeV). Separation of the slow, highly ionizing helium nuclei from the high flux of π, p, and d was made by measuring energy loss in and time-of-flight (TOF) between two planes of scintillator counters placed in the 8 GeV spectrometer. The elastic events were identified mainly by the relative TOF between the scattered electrons and the recoil nuclei. This experimental arrangement allowed a measurement free of background even in regions of extremely small cross section.

The event data (all electron triggers)[23] were recorded on tape. In the analysis of the double arm data, corrections were made for dead time, track efficiency in the 20-GeV system, absorption and scattering of the recoil nuclei in the target and scintillators. The radiative corrections were determined in part from a detailed Monte Carlo model of the double arm system including soft photon radiation[14]. The factors independent of ΔE were calculated according to Ref. 15. A liquid hydrogen target was used to calibrate the entire system against the world e-p cross sections.

The open points in Fig. 1 show the electron single arm missing mass spectrum from ^{3}He at $q^2 = 1.4$ (GeV/c)^2 centered at $M_{^3He}^2 = 7.88$ (GeV/c^2)^2 and extended to the limits of the 20-GeV spectrometer acceptance. The events at small missing mass come from the target end windows and the ^{4}He contamination, and those at large missing mass come from inelastic scattering. The closed points represent the double arm e-^{3}He coincidence spectrum and clearly show only the elastic peak and its radiative tail.

The cross section for e-^{3}He scattering is written:

$$\frac{d\sigma}{d\Omega} = \sigma_M \left[F_{ch}^2 + F_{mag}^2 \mu^2 \tau \left[1 + 2(1 + \tau)\tan^2(\theta/2) \right] \right] \Big/ (1+\tau)$$

$$= \sigma_M \left[A(q^2) + B(q^2) \tan^2(\theta/2) \right]$$

and for ^{4}He

$$\frac{d\sigma}{d\Omega} = \sigma_M \, F_{ch}^2 = \sigma_M \, A(q^2)$$

where σ_M is the Mott cross section for scattering from a spinless point nucleus, F_{ch} and F_{mag} are the charge and magnetic form factors, θ is the electron scattering angle, $\tau = q^2/4M^2$, M is the target mass, and $\mu = -3.2\mu_N$ is the nuclear magnetic moment. We will assume that at our scattering angle of 8° the cross section for ^{3}He is entirely due to the $A(q^2)$ term. The $B(q^2)$ term is greatly suppressed and would contribute less than 1.0% for $F_{ch} = F_{mag}$.

The numerical results for our experiment are listed in Table I and plotted in Figs. 2 and 3. The errors quoted are the statistical error plus 5% systematic error added linearly. For ^{3}He our data show the structure function $A^{\frac{1}{2}}(q^2)$ falling smoothly over 2 decades up to $q^2 = 2.5$ (GeV/c)^2. For larger momentum transfer, it is not clear whether we observe a diffraction feature or not; at a

cross section of 5×10^{-39} cm^2/sr ($A^{\frac{1}{2}} = 3 \times 10^{-5}$) we have reached our level of sensitivity of 1 event in 5 Coulombs (about 6 days of running). An empirical fit to the data for $q^2 \geq 0.7$ (GeV/c)^2 using $A^{\frac{1}{2}}(q^2) = ae^{-bq^2}$ gives $a = 0.034 \pm 0.004$ and $b = 2.72 \pm 0.09$ with a reduced chi square of 1.03 indicating that the new data are compatible with the absence of a diffraction feature.

The ^{4}He charge form factor is quite similar and falls off more quickly than ^{3}He with increasing q^2. A fit using the exponential function for $q^2 \geq 0.8$ (GeV/c)^2 gives $a = 0.14 \pm 0.03$ and $b = 4.0 \pm 0.2$ with a reduced chi square of 1.40. The steepening decline of F_{ch} near $q^2 = 1.8$ and the worse fit suggests the presence of a second diffraction minimum, but we have not been able to measure a value for F_{ch} at the momentum transfer $q^2 = 2.4$ (GeV/c)^2 which we conjecture to be the position of the next diffraction maximum.

Figure 2 shows calculations of F_{ch} and $A^{\frac{1}{2}}$ for ^{3}He from various microscopic and asymptotic models. The solid curve is the one-body form factor F_{ch} from a Faddeev calculation[16] in momentum space. The result from a Faddeev calculation[17] in configuration space, shown by the dotted curve, is almost indistinguishable from the solid curve up to $q^2 = 2.2$ (GeV/c)^2. Both of these calculations used the Reid soft core (RSC) interaction for the nucleon-nucleon force, and nucleon form factors from Ref. 18. The calculation of Ref. 5 is also very similar up to $q^2 = 2.0$ (GeV/c)^2, the main difference being a diffraction maximum near $q^2 = 0.8$ (GeV/c)^2 20% higher. The dot-dashed curve represents the sum of the one-body form factor[16] F_{ch} plus contributions due to meson exchange currents (MEC)[9]. This calculation includes contributions from the pair, and ρ-π current, and includes form factors at the π-N vertices. A calculation using a different one-body density and MEC[19] (not shown) gives results up to $q^2 = 2$ (GeV/c)^2 which are about a factor of 1.4 to 2 higher than the dot-dashed curve from

$q^2 = 0.6$ to 2.0 $(GeV/c)^2$. The small-dashed curve is a prediction[12] for $A^{\frac{1}{2}}$ based on the dimensional-scaling-quark model (DSQM) obtained using a constituent interchange with binding corrections necessary in the preasymptotic region. The pure DSQM is expected to work for truly asymptotic q^2 where it predicts the shape $A^{\frac{1}{2}}(q^2) \propto (q^2)^{1-3A}$ but not the normalization. The large-dashed curve represents $A^{\frac{1}{2}}$ from a calculation[20] that uses a relativistic impulse approximation model (Relativistic IA); it has the same asymptotic fall-off as the DSQM and also gives a good fit to the deuteron structure function and many other inclusive high energy nuclear reactions.

Upon comparing these curves to the new data we can make the following observations. Without experimental measurements[21] or theoretical calculations[22] of F_{mag} for $q^2 \gtrsim 0.8$ $(GeV/c)^2$ it is difficult to test the Faddeev calculations for F_{ch}. If those calculations are correct, $F_{mag} \approx 4 \times F_{ch}$ would be necessary to give the measured value of $A^{\frac{1}{2}}$ near $q^2 = 1.5$ $(GeV/c)^2$ and F_{mag} could fill in the second diffraction minimum in F_{ch}. If we assume F_{mag} is small, the old discrepancy for the Faddeev calculations in the height of the second maximum in the region of $q^2 = 0.8$ $(GeV/c)^2$ is seen to continue at about the same level out to $q^2 = 2.0$ $(GeV/c)^2$. The contribution of meson exchange currents, at least in their present form, improves the agreement around $q^2 = 0.8$ $(GeV/c)^2$. Since the MEC contributions in the region of $q^2 = 0.8$ $(GeV/c)^2$ vary slowly with q^2, whereas the one-body form factor shows pronounced structure, we tend to assign the disagreement at $q^2 = 0.8$ $(GeV/c)^2$ to a one-body form factor which is too small. The apparent disagreement in the region of $q^2 = 2$ $(GeV/c)^2$ is due to a complicated mixture of many effects and interpretation of this region will take more careful study.

The dimensional-scaling-quark model falls more slowly than the data as a function of q^2. This indicates that even with the mass correction employed, scaling sets in at a q^2 considerably larger than expected. The lower limit for the onset of scaling in this form is $q^2 \approx 2.2$ $(GeV/c)^2$. The relativistic impulse approximation of Ref. 20 does not attempt to describe the diffractive structure at low q^2, but it seems to agree fairly well with the data in the preasymptotic region.

Theoretical calculations of F_{ch} for ^{4}He are shown in Fig. 3. The dotted curve[11] is a calculation based on Faddeev-Bruckner-Hartree-Fock (FBHF) theory employing the RSC interaction, and includes contributions from the MEC terms coming from pair and pionic current graphs including π-N form factors. The solid curve has been obtained[9] using a simplified one-body wave function of Gaussian form with Jastrow correlation factors in order to study the effect of MEC contributions. The dashed curve[12] and the large-dashed curve[20] in Fig. 3 are the scaling predictions analogous to the ones discussed above for ^{3}He. The theoretical description of ^{4}He is not as fully developed as that for ^{3}He, however, the discrepancies between the curves presented in Fig. 3 and the new data is similar to that observed for ^{3}He.

The new data on helium form factors at large q^2 indicate that the existing microscopic calculations of the wave functions are missing an important ingredient. The comparison with the scaling predictions shows that until now only the pre-asymptotic region of the structure functions has been explored. For large q^2 both theoretical predictions and experimental measurements of F_{mag} for ^{3}He are called for.

REFERENCES

1. J. S. McCarthy, I. Sick, R. R. Whitney, Phys. Rev. $\underline{C15}$, 1396 (1977) and references therein for low q data. M. Bernheim, D. Blum, W. McGill, R. Riskalla, C. Trail, T. Stovall, D. Vinciguerra, Lett. Nuovo Cim $\underline{5}$, 431 (1972). R. F. Frosch, J. S. McCarthy, R. E. Rand, M. R. Yearian, Phys. Rev. $\underline{160}$, 1308 (1966).

2. R. G. Arnold, B. T. Chertok, E. B. Dally, A. Grigorian, C. L. Jordan, W. P. Schütz, R. Zdarko, F. Martin, B. A. Mecking, Phys. Rev. Lett. $\underline{35}$, 776 (1975).

3. A. D. Jackson, A. Lande, P. U. Sauer, Nucl. Phys. $\underline{A156}$, 1 (1970).

4. L. M. Delves, M. A. Hennell, Nucl. Phys. $\underline{A168}$, 347 (1971), $\underline{A246}$, 490 (1975).

5. M. R. Strayer, P. U. Sauer, Nucl. Phys. $\underline{A231}$, 1 (1974).

6. R. A. Brandenburg, Y. E. Kim, A. Tubis, Phys. Rev. $\underline{C12}$, 1368 (1975). A. E. L. Dieperink, T. deForest, I. Sick, R. A. Brandenburg, Phys. Lett. $\underline{63B}$, 261 (1976).

7. A. Laverne, C. Gignoux, Phys. Rev. Lett. $\underline{29}$, 436 (1972).

8. W. M. Kloet, J. A. Tjon, Phys. Lett. $\underline{49B}$, 419 (1974); Phys. Lett. $\underline{61B}$, 356 (1976).

9. J. Borysowicz, D. O. Riska, Nucl. Phys. $\underline{A254}$, 301 (1975), and MSU internal report.

10. M. Radomski, D. O. Riska, Nucl. Phys. A274, 428 (1976).

11. M. Gari, H. Hyuga, J. G. Zabolitzky, Nucl. Phys. $\underline{A271}$, 365 (1976).

12. S. J. Brodsky, B. T. Chertok, Phys. Rev. $\underline{D14}$, 3003 (1976).

13. S. Stein, W. B. Atwood, E. D. Bloom, R. L. A. Cottrell, H. DeStabler, C. L. Jordan, H. G. Piel, C. Y. Prescott, R. Siemann, R. E. Taylor, Phys. Rev. $\underline{D12}$, 1884 (1975).

14. G. Miller, Thesis (unpublished), SLAC Report No. SLAC-129 (1971).

15. Y. S. Tsai, SLAC-PUB-848, Jan. 1971 and L. W. Mo and Y. S. Tsai, Rev. Mod. Phys. <u>41</u>, 205 (1969).

16. Calculated by I. Sick from wave functions of Ref. 6 supplied by R. A. Brandenburg via private communication.

17. Calculated by I. Sick from the point density of Ref. 7 obtained by private communication.

18. S. Blatnik, N. Zovko, Acta Phys. Austriaca <u>39</u>, 62 (1974).

19. E. Hadjimichael, preprint, Fairfield University, Fairfield, Conn. 06430.

20. I. A. Schmidt, R. Blankenbecler, Phys. Rev. <u>D15</u>, 3321 (1977), SLAC-PUB-1931, May 1977, and I. A. Schmidt, SLAC-Report-203 (thesis), August 1977.

21. F_{mag} for ^{3}He is experimentally not known above $q^2 = 0.6$ $(GeV/c)^2$, Bernheim et al, Ref. 1.

22. See A. Barroso and E. Hadjimichael, Nucl. Phys. <u>A238</u>, 422 (1975) and references therein for calculations of F_{mag} up to $q^2 = 0.8$ $(GeV/c)^2$.

23. Single arm electron spectra in the threshold region of quasielectric scattering will be presented in a future publication.

TABLE 1

Structure Function Results for ^{3}He and ^{4}He

q^2 (GeV/c)^2	^{3}He $\left| A^{\frac{1}{2}} \right| \times 10^{-3}$	^{4}He $\left| F_{ch} \right| \times 10^{-3}$
0.7	4.57 ± .015	
0.8	3.56 ± 0.32	5.49 ± 0.60
1.0	2.28 ± 0.23	2.41 ± 0.22
1.2	1.42 ± 0.13	1.36 ± 0.19
1.4	0.817 ± 0.073	0.579 ± 0.098
1.6	0.456 ± 0.045	0.273 ± 0.063
1.8	0.275 ± 0.039	0.065 ± 0.025
2.0	0.108 ± 0.025	-
2.25	0.056 ± 0.017	-
2.4	-	≤ 0.043
2.5	0.028 ± .015	-
3.0	0.032 ± .018	-
4.0	≤ 0.057	

FIGURE CAPTIONS

1. Electron missing mass spectra from ^{3}He. Open circles represent total scattered electrons. Closed circles represent scattered electrons in coincidence with recoil ^{3}He.

2. Results of this and previous experiments for ^{3}He structure function $A^{\frac{1}{2}}$ displayed with theoretical predictions of F_{ch} and $A^{\frac{1}{2}}$. The curves (described in the text) are solid: F_{ch} Faddeev (Ref. 16), dotted: F_{ch} Faddeev (Ref. 17), dot dashed: Sum of Faddeev one-body (Ref. 16) plus MEC (Ref. 9), small dashed: $A^{\frac{1}{2}}$ DSQM (Ref. 12); large dashed: $A^{\frac{1}{2}}$ Relativistic IA (Ref. 20).

3. Results of this and previous experiments for ^{4}He charge form factor F_{ch} displayed with theoretical predictions. The curves are (see text), solid: F_{ch} Gaussian one-body with Jastrow correlation plus MEC (Ref. 9), dotted: F_{ch} FBHF plus MEC (Ref. 11), small dashed: $A^{\frac{1}{2}}$ DSQM (Ref. 12), large dashed: A Relativistic IA (Ref. 20).
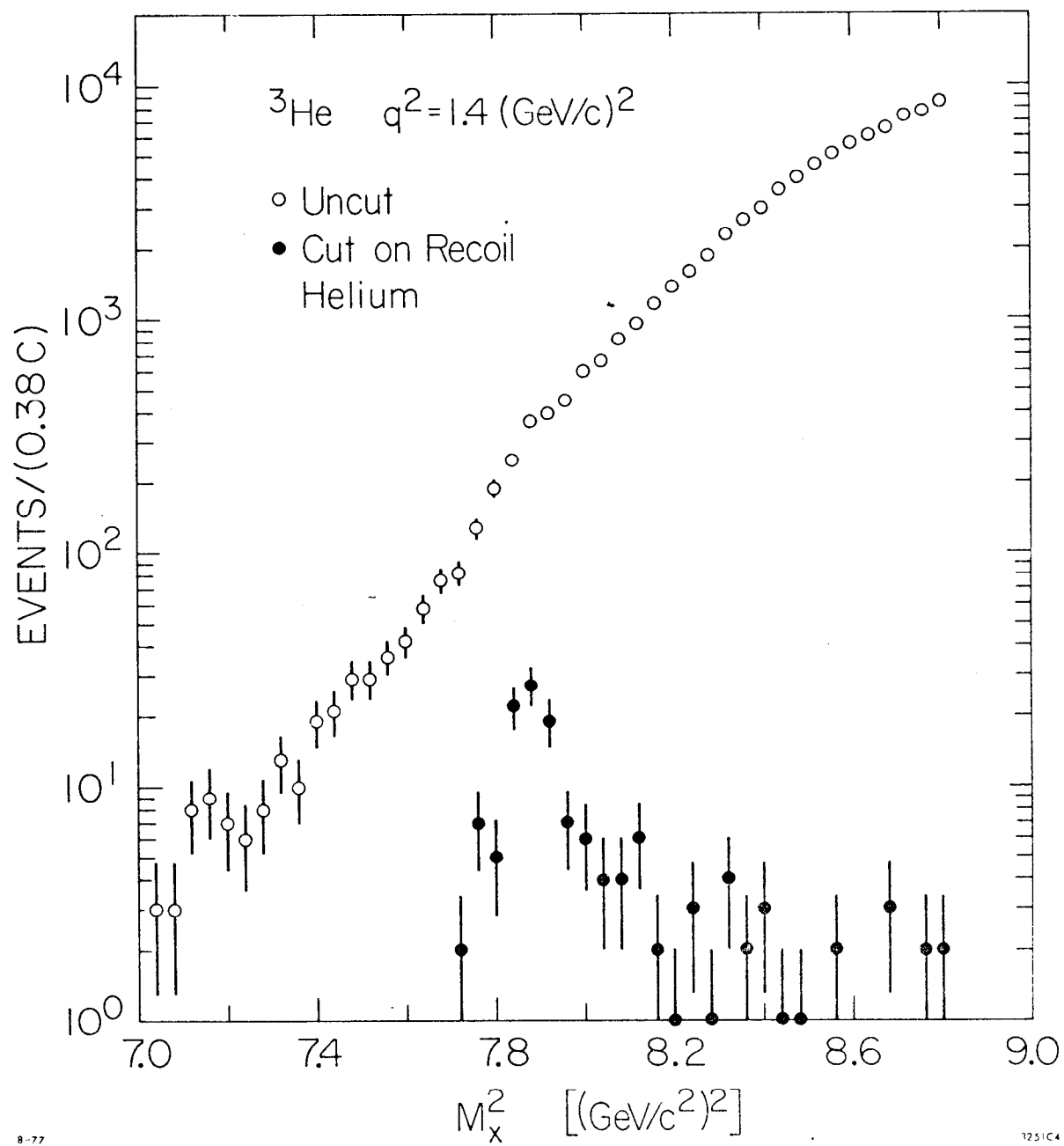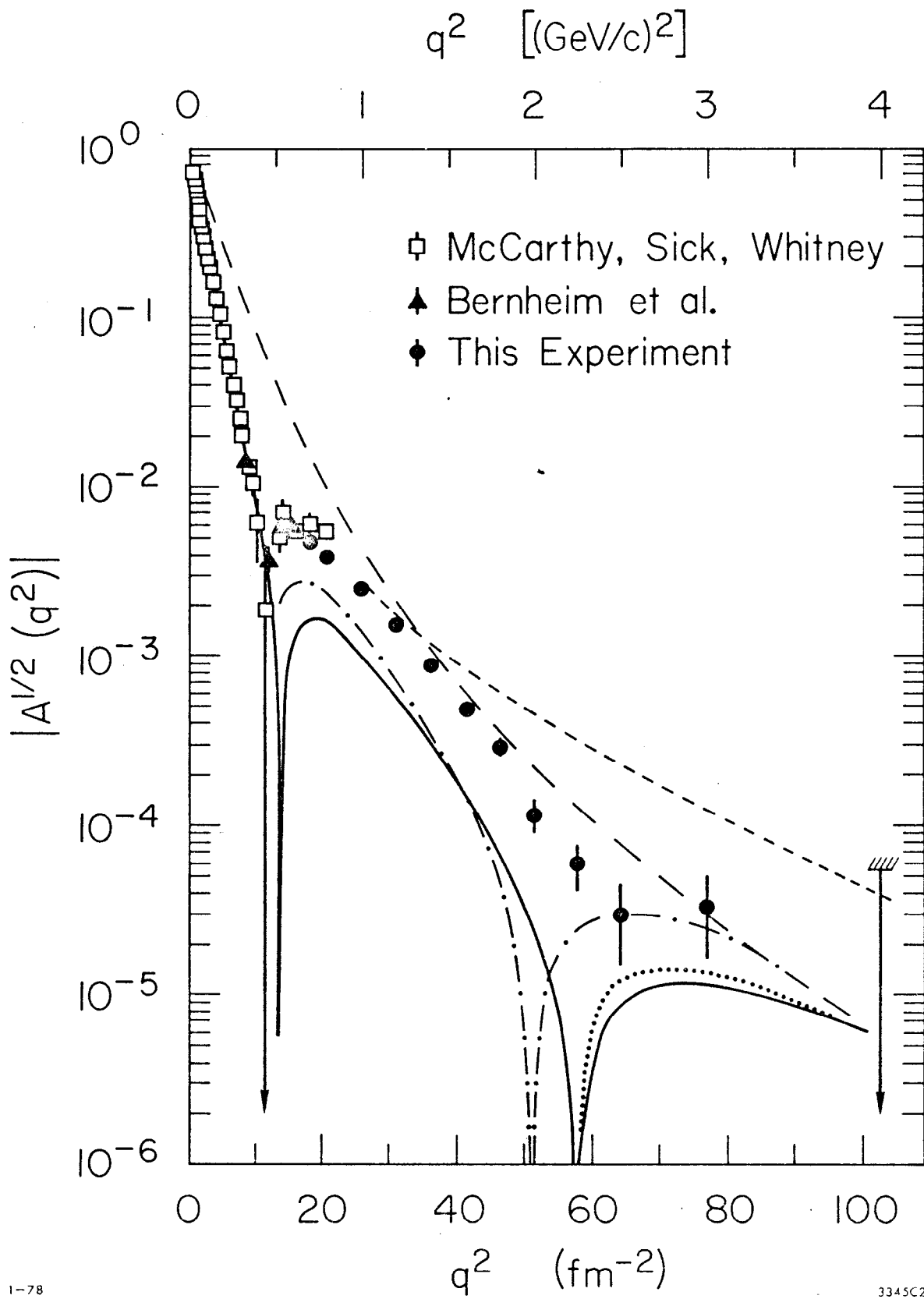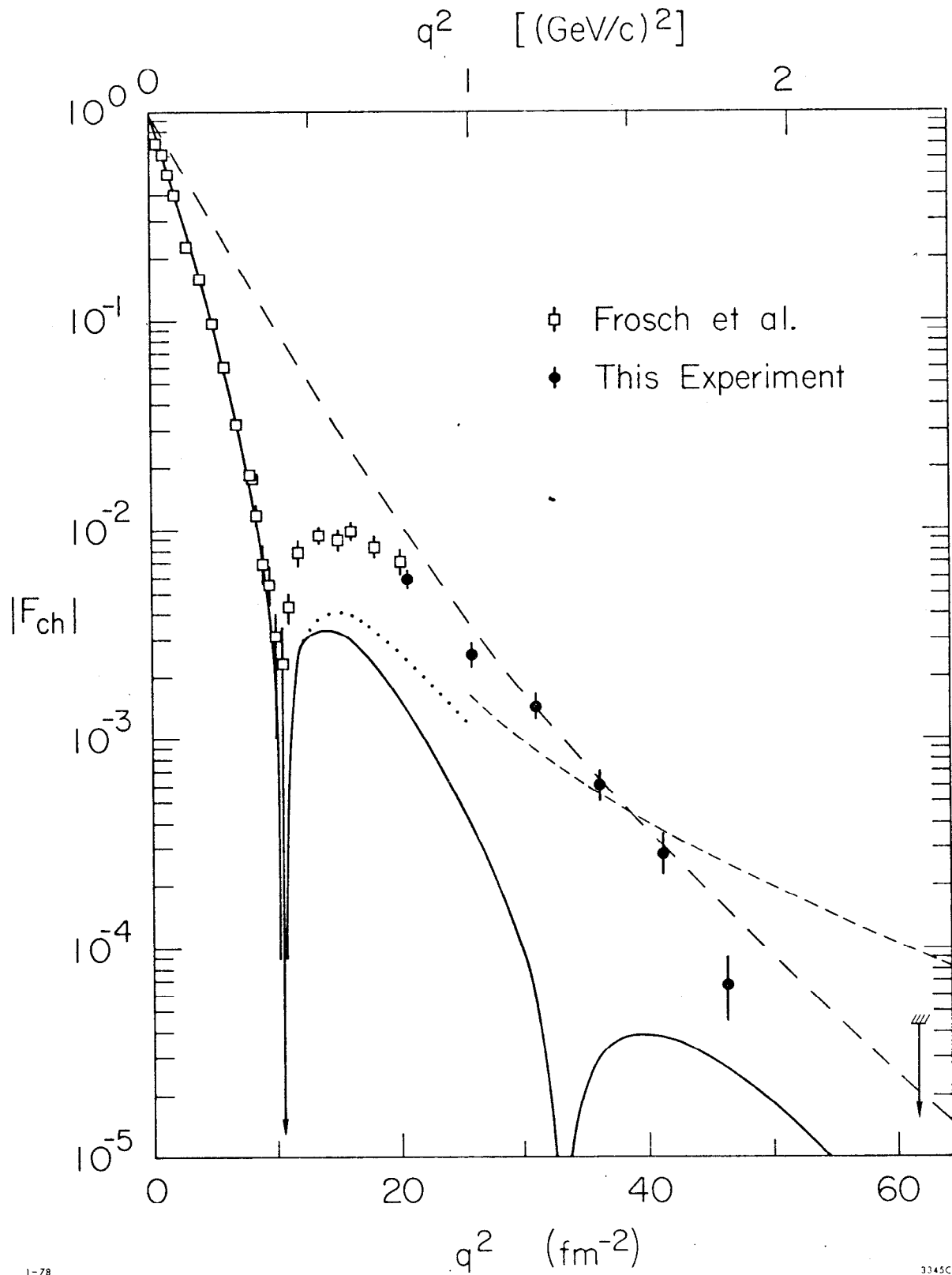
Fig. 1

Fig. 2

1-78

3345C2

Fig. 3